Stress Singularity of the Obtuse Notch Tip for the Case of a Notch lying along the Bi-material Interface

Takeshi Tane[1,*], Takeshi Uchida[1], Toru Sasaki[2] and Hiroki Hamano[3]

[1]Department of Mechanical Engineering, Kitakyushu National College of Technology, Kitakyushu, Japan

[2]Department of Mechanical Engineering, Nagaoka University of Technology, Nagaoka, Japan

[3]A professor emeritus at the Matsue National College of Technology, Matsue, Japan

Abstract: The authors have previously studied the stress singularities for a crack tip with various open cracks meeting at the interface between different materials for plane problems. Based on these results, this paper deals with the linear elastic stress fields near a crack and smooth notch that lie along the interface of two dissimilar materials. An analytical solution for the crack and notch tip is given in general terms according to Muskhelishvili's method based on complex stress functions. Arbitrary constants of those functions are determined by the boundary conditions for stresses along the notch surface and continuity conditions for stresses and displacements on the interface. By using Bogy's method, α-β lines are shown for various open cracks and smooth notches. Also, it is found that these equations agree with the foregone solutions of Lin & Mar and the authors.

Keywords: Stress singularity, Smooth notch, Dundurs' parameter, Fracture mechanics.

1. Introduction

Stress concentrations are caused along the interface of dissimilar materials, cracks, and notches. Because many structures are designed for safety, it is important to obtain the stress distributions at these positions.

The authors already presented several solutions for stress singularities using two-dimensional elastic theory for isotropic and anisotropic composite materials [1], [2]. For example, stress singularities for a notch, which has opening angles and is at the interface of three dissimilar isotropic materials, are discussed considering the continuity conditions for stresses and displacements at the interfaces and the boundary conditions for stresses on the notch surface.

Generally speaking, a notch tip has no tip radius [3]-[5], but this study allowed a notch tip radius. In this paper, such notches are called smooth notches. Singular solutions are calculated for a smooth notch with an opening angle and where the notch meets the interface of two dissimilar materials. It is assumed that the regional angles of both materials are equal and that both materials behave as isotropic bodies.

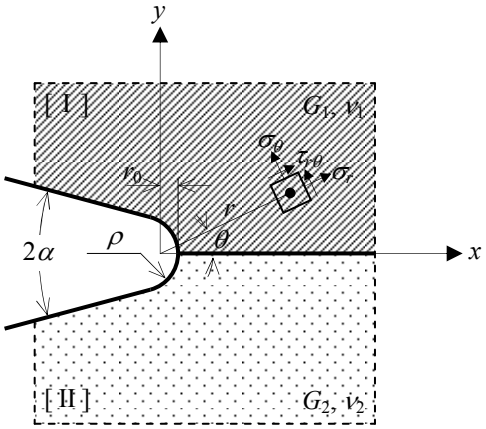

Fig. 1 Coordinate system.

2. Analytical theory

2.1 *Basic equations of elastic mechanics*

First, the equilibrium equations for two-dimensional problems without body forces are shown in the polar coordinate system (r, θ) as follows:

*Corresponding author: E-mail: tane@kct.ac.jp; Tel: +81-93-964-7264; Fax: +81-93-964-7264

$$\frac{\partial \sigma_r}{\partial r}+\frac{1}{r}\frac{\partial \tau_{r\theta}}{\partial \theta}+\frac{\sigma_r-\sigma_\theta}{r}=0,\ \frac{\partial \tau_{r\theta}}{\partial r}+\frac{1}{r}\frac{\partial \sigma_\theta}{\partial \theta}+\frac{2\tau_{r\theta}}{r}=0. \tag{1}$$

Second, the geometrical equations, which characterize the relationship between strains and displacements, are obtained:

$$\varepsilon_r=\frac{\partial u_r}{\partial r},\ \varepsilon_\theta=\frac{1}{r}\frac{\partial u_\theta}{\partial \theta}+\frac{u_r}{r},\ \gamma_{r\theta}=\frac{\partial u_\theta}{\partial r}+\frac{1}{r}\frac{\partial u_r}{\partial \theta}-\frac{u_\theta}{r}, \tag{2}$$

where u_r and u_θ are the displacements in the r and θ directions, respectively.

Third, the constitutive equations for an isotropic elastic body in a two-dimensional problem are

$$\varepsilon_r=\frac{1}{E}(\sigma_r-\nu\sigma_\theta),\ \varepsilon_\theta=\frac{1}{E}(\sigma_\theta-\nu\sigma_\rho),\ \gamma_{r\theta}=\frac{\tau_{r\theta}}{G}, \tag{3}$$

for plane stress, where E and ν are the Young's modulus and Poisson's ratio, respectively, and $G = E/(1 + \nu)$ is the shear modulus of the material.

2.2 *Governing equation and general solution*

From Eq. (2), the strain components must satisfy the following compatibility equation of strain:

$$\frac{\partial^2 \varepsilon_\theta}{\partial r^2}+\frac{2}{r}\frac{\partial \varepsilon_\theta}{\partial r}+\frac{1}{r^2}\frac{\partial^2 \varepsilon_r}{\partial \theta^2}-\frac{1}{r}\frac{\partial \varepsilon_r}{\partial r}-\frac{1}{r}\frac{\partial^2 \gamma_{r\theta}}{\partial r\partial \theta}-\frac{1}{r^2}\frac{\partial \gamma_{r\theta}}{\partial \theta}=0. \tag{4}$$

Also, introducing Airy's stress function $F(r,\theta)$, which satisfies Eq. (1) automatically, the stress components in Eq. (1) are denoted as

$$\sigma_r=\frac{1}{r}\frac{\partial F}{\partial r}+\frac{1}{r^2}\frac{\partial^2 F}{\partial \theta^2},\ \sigma_\theta=\frac{\partial^2 F}{\partial r^2},\ \tau_{r\theta}=-\frac{1}{r}\frac{\partial^2 F}{\partial r\partial \theta}+\frac{1}{r^2}\frac{\partial F}{\partial \theta}. \tag{5}$$

Substituting Eq. (5) into Eq. (3) and then substituting the obtained equation into Eq. (4), the stress function F must satisfy the following partial differential equation [6]:

$$\nabla^2\nabla^2 F=0, \tag{6}$$

where

$$\nabla^2=\frac{\partial^2}{\partial r^2}+\frac{1}{r}\frac{\partial}{\partial r}+\frac{1}{r^2}\frac{\partial^2}{\partial \theta^2}. \tag{7}$$

The solution of the biharmonic equation (6) is expressed using Goursat's complex stress functions $\phi(z)$ and $\psi(z)$ as

$$F(r,\theta)=\mathrm{Re}[\bar{z}\phi(z)+\psi(z)], \tag{8}$$

where $z = x + i\,y = re^{i\theta}$, and $\bar{z}$ is its complex conjugate. These functions, $\phi(z)$ and $\psi(z)$, are determined by taking into account the boundary conditions for the stresses or displacements of each elastic problem.

2.3 *Formula for the stress and displacement components of an isotropic elastic material*

By using complex stress functions, the stress and displacement components of an isotropic material are given by

$$\left.\begin{aligned}&\sigma_r+\sigma_\theta=4\,\mathrm{Re}[\phi'(z)],\\&\sigma_\theta-\sigma_r+2i\tau_{r\theta}=2e^{2i\theta}[\bar{z}\phi'(z)+\psi'(z)],\\&2G(u_r+iu_\theta)=e^{-i\theta}[\kappa\phi(z)-z\overline{\phi'(z)}-\overline{\psi(z)}],\end{aligned}\right\} \tag{9}$$

where

$$\kappa=\begin{cases}3-4\nu & \text{for plane strain},\\ (3-\nu)/(1-\nu) & \text{for plane stress}.\end{cases} \tag{10}$$

3. Analytical approach

3.1 *Mapping function*

This paper presents an analytical solution for Fig. 1. However, because of the difficulty of applying boundary conditions for stresses on a U-shape notch, the following mapping function is introduced [7]:

$$z=x+iy\equiv f(w)=w^q=(u+iv)^q. \tag{11}$$

In this equation, the exponent q is related to the opening angle 2α [rad] and is expressed as

$$q = 2 - \frac{2\alpha}{\pi}. \tag{12}$$

For example, if $2\alpha = 0$, then $q = 2$, if $2\alpha = \pi$, then $q = 1$, and so on.

By introducing the mapping function expressed in Eq. (11), the focusing length r_0 shown in Fig. 1 is represented by the radius of curvature ρ as the following equation:

$$r_0 = \frac{q-1}{q}\rho. \tag{13}$$

As an example, Fig. 2 shows the mapping results for the case of $2\alpha = 30$ deg. The radius of curvature ρ is changed from 0 to 10 for descriptive purposes. In particular, it is noted that the curvature for the case of $\rho = 0$ (i.e., $r_0 = 0$) coincides with a V-shape notch with an opening angle of 2α, which was studied by Kato and Fujitani [5].

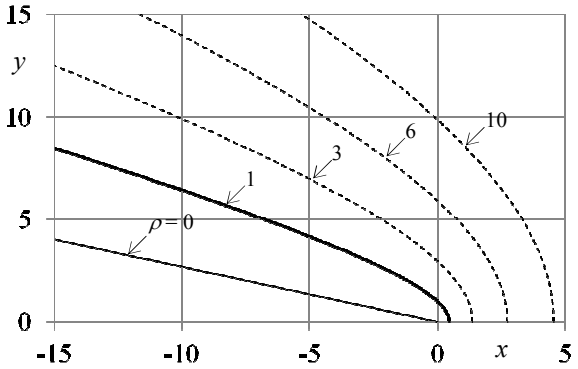

Fig. 2 Map transformation from (u, v) coordinate system to (x, y) coordinate system for the case of a notch opening angle of $2\alpha = 30$ deg.

3.2 *Complex stress function*

In this paper, Goursat's stress functions are assumed to be power functions of the complex variable z, i.e.,

$$\phi_j(z) = a_j z^{\lambda}, \ \psi_j(z) = b_j z^{\lambda} + c_j z^{\mu}. \tag{14}$$

The subscript j (= 1 or 2) indicates the analytical region. The exponents λ and μ in Eq. (14) are both complex, and these constants are determined from the traction-free condition on a U-notch surface and the continuity conditions of stresses and displacements on the bi-material interfaces shown in Fig. 1.

3.3 *Formulations for determining stresses and displacements*

By substituting Eq. (14) into Eq. (9), the stresses and displacements of each region are expressed as follows:

$$\left.\begin{aligned}
\sigma_r^j = \ & \lambda r^{\lambda-1}[(3-\lambda)\{a_1^j \cos(1-\lambda)\theta + a_2^j \sin(1-\lambda)\theta\} \\
& - \{b_1^j \cos(1+\lambda)\theta - b_2^j \sin(1+\lambda)\theta\}] \\
& - \mu r^{\mu-1}[c_1^j \cos(1+\mu)\theta - c_2^j \sin(1+\mu)\theta], \\
\sigma_\theta^j = \ & \lambda r^{\lambda-1}[(1+\lambda)\{a_1^j \cos(1-\lambda)\theta + a_2^j \sin(1-\lambda)\theta\} \\
& + \{b_1^j \cos(1+\lambda)\theta - b_2^j \sin(1+\lambda)\theta\}] \\
& + \mu r^{\mu-1}[c_1^j \cos(1+\mu)\theta - c_2^j \sin(1+\mu)\theta], \\
\tau_{r\theta}^j = \ & \lambda r^{\lambda-1}[(1-\lambda)\{a_1^j \sin(1-\lambda)\theta - a_2^j \cos(1-\lambda)\theta\} \\
& + \{b_1^j \sin(1+\lambda)\theta + b_2^j \cos(1+\lambda)\theta\}] \\
& + \mu r^{\mu-1}[c_1^j \sin(1+\mu)\theta + c_2^j \cos(1+\mu)\theta],
\end{aligned}\right\} \tag{15}$$

$$\left.\begin{aligned} 2G_j u_r^j = \; & r^{\lambda}[(\kappa_j-\lambda)\{a_1^j\cos(1-\lambda)\theta + a_2^j\sin(1-\lambda)\theta\} \\ & -\{b_1^j\cos(1+\lambda)\theta - b_2^j\sin(1+\lambda)\theta\}] \\ & -r^{\mu}[c_1^j\cos(1+\mu)\theta - c_2^j\sin(1+\mu)\theta], \\ 2G_j u_\theta^j = & -r^{\lambda}[(\kappa_j+\lambda)\{a_1^j\sin(1-\lambda)\theta - a_2^j\cos(1-\lambda)\theta\} \\ & -\{b_1^j\sin(1+\lambda)\theta + b_2^j\cos(1+\lambda)\theta\}] \\ & +r^{\mu}[c_1^j\sin(1+\mu)\theta + c_2^j\cos(1+\mu)\theta], \end{aligned}\right\} \tag{16}$$

where a_1^j and a_2^j are the real and imaginary parts of the complex constants a_j (j = 1, 2), respectively. Thus, $a_j = a_1^j + i\,a_2^j$. Similarly, $b_j = b_1^j + i\,b_2^j$ and $c_j = c_1^j + i\,c_2^j$.

3.4 *Transformation of the stresses*

The next transformational expressions are introduced by applying the boundary conditions for the stresses mentioned below. That is, the stress components in curvilinear coordinates (u, v) shown in Fig. 2 are obtained as

$$\left.\begin{aligned} \sigma_u^j &= \frac{\sigma_r^j+\sigma_\theta^j}{2} + \frac{\sigma_r^j-\sigma_\theta^j}{2}\cos\frac{2\theta}{q} - \tau_{r\theta}^j\sin\frac{2\theta}{q}, \\ \sigma_v^j &= \frac{\sigma_r^j+\sigma_\theta^j}{2} - \frac{\sigma_r^j-\sigma_\theta^j}{2}\cos\frac{2\theta}{q} + \tau_{r\theta}^j\sin\frac{2\theta}{q}, \\ \tau_{uv}^j &= \frac{\sigma_r^j-\sigma_\theta^j}{2}\sin\frac{2\theta}{q} + \tau_{r\theta}^j\sin\frac{2\theta}{q}, \end{aligned}\right\} \tag{17}$$

where the stress components on the right side are given in polar coordinates (r, θ) and are computed easily from Eq. (15).

4. Evaluation of λ parameters

4.1 *Boundary conditions and continuity conditions*

First, the boundary conditions for the stress components σ_u and τ_{uv} in Eq. (17) on a U-notch surface are represented as

$$(\sigma_u^j)_{u=u_0} = 0, \quad (\tau_{uv}^j)_{u=u_0} = 0, \tag{18}$$

by taking into account the traction-free conditions on the surface. In particular, the above conditions are reduced to the following equations far away from the notch tip by considering Eq. (17):

$$(\sigma_u^j)_{\substack{u=u_0 \\ |v|>>u_0}} = 0 \;\Rightarrow\; \left.\begin{aligned} &\lim_{\substack{r\to\infty \\ \theta\to+q\pi/2}} (r^{1-\lambda}\sigma_\theta^1) = 0, \\ &\lim_{\substack{r\to\infty \\ \theta\to-q\pi/2}} (r^{1-\lambda}\sigma_\theta^2) = 0, \end{aligned}\right\} \tag{19}$$

$$(\tau_{uv}^j)_{\substack{u=u_0 \\ |v|>>u_0}} = 0 \;\Rightarrow\; \left.\begin{aligned} &\lim_{\substack{r\to\infty \\ \theta\to+q\pi/2}} (r^{1-\lambda}\tau_{r\theta}^1) = 0, \\ &\lim_{\substack{r\to\infty \\ \theta\to-q\pi/2}} (r^{1-\lambda}\tau_{r\theta}^2) = 0. \end{aligned}\right\} \tag{20}$$

On the other hand, Eq. (18) leads to the following equations at the U-notch tip:

$$(\sigma_u^j)_{\substack{u=u_0 \\ v=0}} = 0 \;\Rightarrow\; \left.\begin{aligned} &(\sigma_r^1)_{\substack{r=r_0 \\ \theta=0}} = (\sigma_r^2)_{\substack{r=r_0 \\ \theta=0}} = 0, \\ &\left(\frac{\partial\sigma_r^1}{\partial\theta}\right)_{\substack{r=r_0 \\ \theta=0}} = \left(\frac{\partial\sigma_r^2}{\partial\theta}\right)_{\substack{r=r_0 \\ \theta=0}} = 0. \end{aligned}\right\} \tag{21}$$

$$\left.\begin{aligned} & (\tau_{r\theta}^{1})_{\substack{r=r_0\\ \theta=0}} = (\tau_{r\theta}^{2})_{\substack{r=r_0\\ \theta=0}} = 0, \\ (\tau_{uv}^{j})_{\substack{u=u_0\\ v=0}} = 0 \;\Rightarrow\; & \left(\frac{\partial \tau_{r\theta}^{1}}{\partial \theta}\right)_{\substack{r=r_0\\ \theta=0}} - \frac{1}{q}(\theta_{\theta}^{1})_{\substack{r=r_0\\ \theta=0}} = \left(\frac{\partial \tau_{r\theta}^{2}}{\partial \theta}\right)_{\substack{r=r_0\\ \theta=0}} - \frac{1}{q}(\theta_{\theta}^{2})_{\substack{r=r_0\\ \theta=0}} = 0. \end{aligned}\right\} \tag{22}$$

Next, the continuity conditions at the two-material interface for stresses and displacements are described as

$$\sigma_{\theta}^{1} = \sigma_{\theta}^{2}, \quad \tau_{r\theta}^{1} = \tau_{r\theta}^{2}, \quad u_{r}^{1} = u_{r}^{2}, \quad u_{\theta}^{1} = u_{\theta}^{2}, \quad \text{at} \quad \theta = 0\,\text{deg}. \tag{23}$$

4.2 *Characteristic equation*

By using the boundary conditions of Eqs. (19) and (20) and the continuity conditions for the case far away from the tip shown in Eq. (23), the simultaneous equations related to eight real constants a_{ij} and b_{ij} (i = 1, 2; j = 1, 2) are derived as

$$\begin{bmatrix} \gamma\cos\phi & \gamma\sin\phi & \cos\psi & -\sin\psi & 0 & 0 & 0 & 0 \\ \delta\sin\phi & -\delta\cos\phi & \sin\psi & \cos\psi & 0 & 0 & 0 & 0 \\ \gamma & 0 & 1 & 0 & -\gamma & 0 & -1 & 0 \\ mP_1 & 0 & -m & 0 & -P_2 & 0 & 1 & 0 \\ 0 & -\delta & 0 & 1 & 0 & \delta & 0 & -1 \\ 0 & mQ_1 & 0 & m & 0 & -Q_2 & 0 & -1 \\ 0 & 0 & 0 & 0 & \gamma\cos\phi & -\gamma\sin\phi & \cos\psi & \sin\psi \\ 0 & 0 & 0 & 0 & -\delta\sin\phi & -\delta\cos\phi & -\sin\psi & \cos\psi \end{bmatrix} \begin{Bmatrix} a_1^1 \\ a_2^1 \\ b_1^1 \\ b_2^1 \\ a_1^2 \\ a_2^2 \\ b_1^2 \\ b_2^2 \end{Bmatrix} = \begin{Bmatrix} 0 \\ 0 \\ 0 \\ 0 \\ 0 \\ 0 \\ 0 \\ 0 \end{Bmatrix}, \tag{24}$$

where

$$\left.\begin{aligned} & P_j = \kappa_j - \lambda, \quad Q_j = \kappa_j + \lambda, \quad \phi = (1-\lambda)q\pi/2, \quad \psi = (1+\lambda)q\pi/2, \\ & \gamma = 1+\lambda, \quad \delta = 1-\lambda, \quad m = G_2/G_1. \end{aligned}\right\}$$

Because the real constants a_{ij}, b_{ij} (i = 1, 2; j = 1, 2) in Eq. (24) are nonzero, the following must be satisfied:

$$\begin{vmatrix} \gamma\cos\phi & \gamma\sin\phi & \cos\psi & -\sin\psi & 0 & 0 & 0 & 0 \\ \delta\sin\phi & -\delta\cos\phi & \sin\psi & \cos\psi & 0 & 0 & 0 & 0 \\ \gamma & 0 & 1 & 0 & -\gamma & 0 & -1 & 0 \\ mP_1 & 0 & -m & 0 & -P_2 & 0 & 1 & 0 \\ 0 & -\delta & 0 & 1 & 0 & \delta & 0 & -1 \\ 0 & mQ_1 & 0 & m & 0 & -Q_2 & 0 & -1 \\ 0 & 0 & 0 & 0 & \gamma\cos\phi & -\gamma\sin\phi & \cos\psi & \sin\psi \\ 0 & 0 & 0 & 0 & -\delta\sin\phi & -\delta\cos\phi & -\sin\psi & \cos\psi \end{vmatrix} = 0, \tag{25}$$

and this determinant is able to express the following characteristic equation:

$$A\beta^2 - 2B\alpha\beta + C\alpha^2 - F = 0, \tag{26}$$

where α and β are called Dundurs' parameters [8] and are represented by

$$\alpha = \frac{(1+\kappa_2) - m(1+\kappa_1)}{(1+\kappa_2) + m(1+\kappa_1)}, \quad \beta = -\frac{(1-\kappa_2) - m(1-\kappa_1)}{(1+\kappa_2) + m(1+\kappa_1)}. \tag{27}$$

A, B, C, and F in Eq. (26) are complex, and they are expressed as

$$\left.\begin{aligned} & A = 4K^2\left(\frac{q\pi}{2}\right), \quad B = 4\lambda^2\sin^2\frac{q\pi}{2}K\left(\frac{q\pi}{2}\right), \\ & C = 4\lambda^2(\lambda^2-1)\sin^4\frac{q\pi}{2}, \quad F = K(q\pi), \end{aligned}\right\} \tag{28}$$

where

$$K(\theta) = \lambda^2 \sin^2\theta - \sin^2(\lambda\theta). \tag{29}$$

If the two regions [I] and [II] in Fig. 1 are made of the same materials, it is noted that Dundurs' parameters α and β are both equal to zero because the numerators of Eq. (28) are both equal to zero. Then, Eq. (26) is reduced as follows [9]:

$$\lambda^2 \sin^2\theta - \sin^2(\lambda\theta) = 0. \tag{30}$$

5. Example calculations

In this section, it is assumed that the ratio of the modulus of rigidity is $m = G_2/G_1$ = 1, 5, 10, 20, 100, and the Poisson's ratios of both materials are 0.30. Figure 3 shows the singular solutions λ derived from Eq. (26) for any aperture angle 2α along the abscissa. These results correspond to the existing results computed by Hamano and Hirashima [1].

For a homogeneous material (i.e., m = 1), the values of λ are always real numbers, which correspond to fracture modes I and II. If $2\alpha = 0$, the stress singularity is $\lambda = 0.5$ as usual.

For an arbitrary ratio of the modulus of rigidity m, except in a homogeneous material (m = 1), the singular solution λ has two real roots or one complex root. From this, it is found that the range of the opening angle 2α (where the singular solution goes from two real solutions to one complex solution) is expanded so that m becomes a large number.

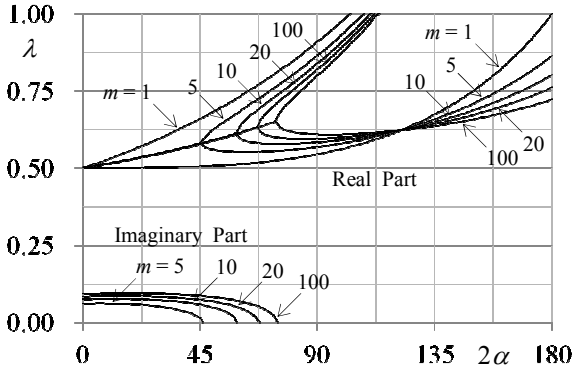

Fig. 3 Singular solution λ versus notch opening angle 2α.

Next, the singular solution λ is shown in Fig. 4 using α-β coordinates, where α and β are Dundurs' parameters expressed in Eq. (27). If the model of Fig. 1 consists of a homogeneous material, the corresponding point on the α-β plane is the origin, i.e., (α, β) = (0, 0). At this point, it is apparent that there are no stress singularities when 2α is greater than or equal to 180 deg. because λ is greater than 1 based on Fig. 4(a)-(c). However, when 2α is less than 180 deg., there is a stress singularity due to the decrease in cross-sectional area near the smooth notch even for a homogeneous material based on Fig. 4(d)-(f). That is, the value of the singular solution λ becomes less than 1.

On the other hand, if the model of Fig. 1 is a common composite material, the corresponding coordinate values on the α-β plane are calculated by Eq. (27) using the ratio of the modulus of rigidity $m = G_2 / G_1$ and the Poisson's ratio. If the opening angle 2α is greater than or equal to 180 deg., a stress singularity may occur at the notch tip because of the combination of materials based on Fig. 4(a)-(c). Also, in this case, the singular solution λ is always a real number. When 2α is less than 180 deg., there are stress singularities for all combinations of the two materials, and the order of the singularity is higher, i.e., the value of the real part of λ approaches 0.5 based on Fig. 4(d)-(f). It is also noted that Fig. 4 corresponds to Bogy's result if the singular solutions are real and corresponds to Koguchi's result if the singular solutions are complex [3], [10].

6. Conclusion

In this paper, stress singularities near the apex of a smooth notch with an arbitrary tip radius ρ that is at a bi-material interface, as shown in Fig. 1, were discussed. For ease of computation, the mapping function expressed in Eq. (11) was introduced, so applying boundary conditions and continuity conditions became very easy.

In the numerical examples, the singular solutions λ were calculated based on the opening notch angle 2α by solving the algebraic equation (26) given by Dundurs' parameters. In the result, these solutions

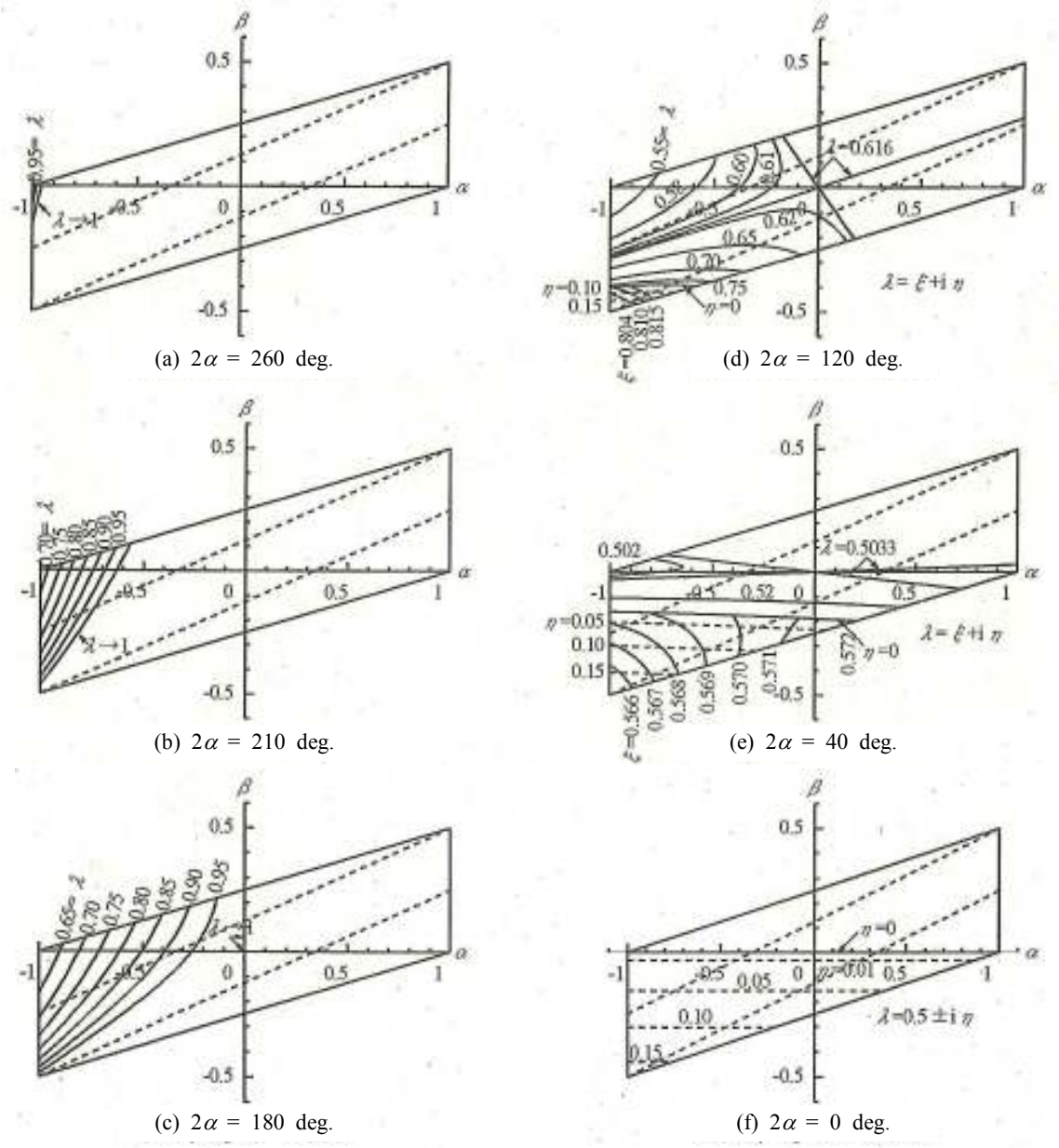

(a) 2α = 260 deg. (d) 2α = 120 deg.

(b) 2α = 210 deg. (e) 2α = 40 deg.

(c) 2α = 180 deg. (f) 2α = 0 deg.

Fig. 4 α-β diagrams for singular solution λ.

coincided with the existing solutions, which were studied by Hirashima and Hamano for composite materials and by Williams for homogeneous materials (i.e., the ratio of the modulus of rigidity is m = 1).

As described in Section 4, because equation (26) does not include the effect of the notch tip shape, the singular solution λ of this study coincides with the existing solution for a V-shape notch. Thus, the effect of the notch tip shape on the stress and displacement distributions of a composite material occurs only in the region near the notch tip.

Next, α-β diagrams were shown for arbitrary opening notch angles 2α, and it was found that these diagrams coincide with Bogy's solution unless the singular solution λ becomes a complex number. If λ is complex, then the α-β diagrams coincide with Koguchi's result.

However, because there are some problems in setting the boundary or continuity conditions, another singular solution μ, which presents the effect of the notch shape, was not determined here. Therefore, the following future areas of study are proposed:

(1) Constructing an analytical technique to obtain the solution μ

(2) Computing the stress and displacement distributions near a smooth notch tip

References

[1] Hirashima K., Hamano H., Hirose Y., Kimura K. Stress singularities in composite materials with an arbitrary open crack meeting an interface: 1st report, the case of a semi-infinite open crack with stress-free surfaces. Transactions of the Japan Society of Mechanical Engineers 1991, Series A; 57(535): 637-644.

[2] Hirashima K., Hamano H., Hirose Y., Kimura K., Koike N. Stress singularities in composite materials with an arbitrary open crack meeting a stress-free, fixed or smooth interface: 2nd report, the cases of a semi-infinite open crack with various boundary conditions such as stress-free, fixed or smooth contact. Transactions of the Japan Society of Mechanical Engineers 1991, Series A; 57(544): 3037-3044.

[3] Bogy D. B. Two edge-bonded elastic wedges of different materials and wedge angles under surface tractions. Journal of Applied Mechanics 1971, Series E; 38(2): 377-386.

[4] Lin K. Y, Mar J. W. Finite element analysis of stress intensity factors for cracks at a bi-material interface. International Journal of Fracture 1976; 12(4): 521-531.

[5] Kato H., Fujitani Y. Analysis of stress singularities and singular solutions at the crack tip in two-dimensional elastic body: Part II, analysis of stress singularities for the crack tip meeting at a bi-material interface. Summaries of Technical Papers of Annual Meeting Architectural Institute of Japan 1984; 59: 1107-1108.

[6] Muskhelishvili N. I. Some basic problems of the mathematical theory of elasticity. Groningen: Noordhoff; 1953.

[7] Lazzarin P., Tovo R. A unified approach to the evaluation of linear elastic stress fields in the neighborhood of cracks and notches. International Journal of Fracture 1996; 78(1): 3-19.

[8] Dundurs J. Discussion of edge-bonded dissimilar orthogonal elastic wedges under normal and shear loading. Journal of Applied Mechanics 1969; 36: 650-652.

[9] Williams M. L. Stress singularities resulting from various boundary conditions in angular corners of plates in extension. Journal of Applied Mechanics 1952; 19(4): 526-528.

[10] Koguchi H., Inoue T., Yada T. Stress singularity near the apex in three-phase bonded structure: effect of the elastic property for intermediate material on the order of the stress singularity. Transactions of the Japan Society of Mechanical Engineers 1993, Series A; 57(535): 637-644.